Transition Boiling Heat Transfer of Droplet Streams and Sprays

John D. Bernardin
Space Sciences and Applications Group,
Los Alamos National Laboratory,
P.O. Box 1663, MS D466,
Los Alamos, NM 87545

Issam Mudawar
Boiling and Two-Phase Flow Laboratory,
School of Mechanical Engineering,
Purdue University,
West Lafayette, IN 47907

An experimental study was performed to characterize the transition boiling heat transfer rate from a surface to a stream of impinging water droplets and to extrapolate this information to predict the transition boiling heat transfer of a dilute spray. First, transition boiling heat transfer data were gathered for a continuous stream of monodispersed water droplets striking a polished nickel surface. From these data, empirical correlations were developed to describe the heat transfer rate and heat transfer efficiency for droplet velocities between $1.0\ \mathrm{m\,s^{-1}}$ *and* $7.1\ \mathrm{m\,s^{-1}}$*, droplet diameters ranging from* 0.250×10^{-3} m to 1.002×10^{-3} m*, and surface temperatures covering* $110-240°\mathrm{C}$*. By properly accounting for the hydrodynamic differences between a spray and a single droplet stream, the empirical single droplet stream heat transfer correlations were effectively extrapolated into a model for predicting the transition boiling heat flux of dilute sprays* ($Q''\approx0.5\times10^{-3}\ \mathrm{m^3\,s^{-1}\,m^{-2}}$)*.* [DOI: 10.1115/1.2764090]

Keywords: droplet, spray, transition boiling, heat transfer

Introduction

The transition boiling heat transfer regime plays an important role in materials processing, power generation, and electronic cooling applications. However, because of its complex and unsteady behavior, it has historically been the least studied of the various boiling regimes. Furthermore, the multifaceted aspects of spray hydrodynamics add further difficulty to the study and understanding of spray transition boiling heat transfer.

The basics of spray boiling heat transfer and the definitions of the four distinct heat transfer regimes are best described by the transient quenching curve, as shown in Fig. 1. At relatively high surface temperatures the film boiling regime exists. In this regime, liquid-solid contact is very brief as the liquid becomes separated from the surface by an insulating vapor layer, resulting in low heat fluxes and slow cooling rates. The lower temperature limit of the film boiling regime is referred to as the Leidenfrost point, which separates the film and transition boiling regimes. Within the transition boiling regime, the liquid droplets make partial and extended contact with the solid surface, as evident by the higher heat fluxes and faster cooling rates. Unique to the transition boiling regime, the heat transfer rate is inversely proportional to the surface temperature. As the surface temperature decreases in the transition boiling regime, the droplet-to-surface contact time increases along with a corresponding increase in the surface heat flux. At the lowest temperature limit of the transition boiling regime, the critical heat flux (CHF) point is encountered. At this point, the liquid droplets make efficient contact with the surface, and boiling heat fluxes as well as cooling rates are at their highest values. Below CHF, the nucleate boiling regime exists. In this regime, the liquid droplets effectively wet the surface and the heat fluxes are large, rapidly decreasing with surface temperature to the lower limit, termed the bubble incipience point. Below this limit, heat transfer occurs by single-phase convection.

Figure 1 is quite general, and the shape of the plot is highly influenced by fluid thermal and hydrodynamic properties, the heated surface characteristics, and surface orientation. Missing from Fig. 1 are the influential aspects of the droplet hydrodynamic parameters including diameter, velocity, frequency, and volumetric flux, as well as the surface properties.

Several qualitative studies have been performed to investigate the many parameters that influence the transition boiling behavior of individual impinging droplets. Chandra and Avedisian [1] used flash photography to investigate the influence of surface temperature on the droplet spreading structure for *n*-heptane droplets impinging upon a polished stainless steel surface. Inada et al. [2], Takeuchi et al. [3], and Makino and Michiyoshi [4] all used high speed photography to study the influence of various droplet and surface parameters on the transition boiling behavior of impinging water droplets. More recently, Bernardin et al. [5,6] used high speed and still photography to develop photographic libraries and droplet regime maps to identify the effects of droplet velocity, surface temperature, and surface roughness on the spreading and heat transfer characteristics of impinging water droplets. Bernardin et al. also made heat transfer measurements to estimate the CHF and Leidenfrost points, the boundaries of the transition boiling regime.

The characterization of droplet heat transfer is typically accomplished by measuring the average heat flux, average heat transfer coefficient, or droplet heat transfer efficiency, the latter of which is defined by

$$\varepsilon=\frac{Q_{\mathrm{sd}}}{Q_{\max}}=\frac{Q_{\mathrm{sd}}}{\rho_f\dfrac{\pi d_0^3}{6}h'_{fg}} \qquad (1)$$

Araki et al. [7] developed an analytical model and incorporated empirical data to estimate the transition boiling heat transfer coefficient for a stream of water droplets impinging upon a heated surface. Inada et al. [2] employed transient temperature measurements and a two-dimensional (2D) analytical model to determine the transition boiling heat flux to impinging water droplets over a wide range of liquid subcooling. Takeuchi et al. [3] and Senda et al. [8] used similar transient quenching techniques of a hot surface by a stream of water droplets to measure the heat transfer rate and heat transfer efficiency over a range of surface temperatures as well as droplet velocities and frequencies.

Deb and Yao [9] used a dimensional analysis to develop the following heat transfer efficiency for a single impinging drop in the transition and film boiling regimes:

$$\varepsilon_{\mathrm{sd}}=0.0273\exp\left[\frac{0.081\sqrt{\ln(\mathrm{We}/35+1)}}{(B+S/60.5)^{1.5}}\right]+0.2109KB\exp\left(\frac{-90}{\mathrm{We}+1}\right) \qquad (2)$$

where the dimensionless parameters are $\mathrm{We}=\rho_f u_o^2 d_o/\sigma$, $B=c_{p,g}(T_s-T_{\mathrm{sat}})/h_{\mathrm{fg}}$, $K=k_g/(c_{p,g}\mu_g)$, and $S=(k\rho c_p)_s^{0.5}/(k\rho c_p)_{\mathrm{steel}}^{0.5}-1$.

The droplet studies discussed here provide important qualitative and quantitative information concerning the heat transfer characteristics of individual droplets. However, they do not provide the tools to directly predict the heat transfer rate of a spray.

Contributed by the Heat Transfer Division of ASME for publication in the JOURNAL OF HEAT TRANSFER. Manuscript received June 22, 2006; final manuscript received February 12, 2007. Review conducted by Ramendra P. Roy. Paper presented at the 2005 ASME International Mechanical Engineering Congress (IMECE2005), Orlando, FL, November 5–11, 2005.

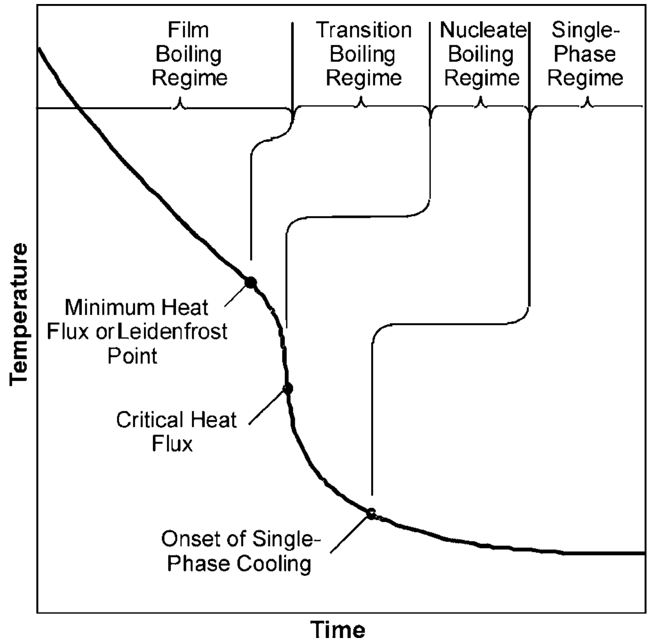

Fig. 1 Temperature-time history of a surface during spray quenching with a subcooled liquid

The primary influential parameters for a transitional boiling heat transfer rate in sprays have been reported to include surface temperature, droplet diameter, droplet velocity, and spray volumetric flux [9–13].

The droplet diameter has been reported to be of minor influence on the spray transition boiling heat flux. Mudawar and Valentine [14] as well as Klinzing et al. [10], using full cone spray nozzles, observed the heat flux to decrease slightly with an increase in droplet Sauter mean diameter over a range of $0.633 \times 10^{-3} - 1.350 \times 10^{-3}$ m. Yao and Choi [13] and Deb and Yao [9], utilizing an impulse droplet atomizer to create a spray of uniform droplets, saw little or no influence of droplet diameter on the transition boiling heat flux.

The transition boiling heat flux was consistently observed to increase with droplet velocity for a variety of studies covering a wide range of spray parameters [9–13]. In all cases, the relationship between the heat flux and droplet velocity was highly nonlinear and very much dependent on the surface temperature and volumetric spray flux.

The second most dominant parameter in spray transition boiling heat transfer is the spray volumetric flux. In Refs. [9,12,13], the effects of volumetric spray flux were isolated by utilizing a monodispersed spray generator to maintain a uniform droplet diameter and velocity while adjusting the volumetric spray flux. From the data presented in those studies, the heat flux appeared to increase linearly with increasing volumetric spray flux ($0.000091 < Q'' < 0.0021$ m^3 s^{-1} m^{-2}). Klinzing et al. [10] employed a full cone spray nozzle and also found heat flux to increase with volumetric spray flux, although the relationship depended on whether the spray was dilute ($Q'' < 0.0035$ m^3 s^{-1} m^{-2}) or dense ($Q'' > 0.0035$ m^3 s^{-1} m^{-2}). It should be noted that although no quantitative categorization of dilute and dense sprays exists, studies [9,10,13,15] have reported liquid volumetric spray flux values in the range of 0.0002–0.0035 m^3 s^{-1} m^{-2} as the boundary between the two spray regimes.

Empirical spray transition boiling heat transfer correlations have been developed for water sprays [10,11,14] over a range of spray conditions. Klinzing et al. [14] presented the following correlation for the transition boiling heat flux q''_{trans}, for full cone water sprays based on local spray hydrodynamic parameters of liquid volumetric flux ($0.6 \times 10^{-3} < Q'' < 9.96 \times 10^{-3}$ m^3 s^{-1} m^{-2}), mean droplet velocity ($10.6 < u_m < 26.5$ m s^{-1}), Sauter mean drop diameter ($0.434 \times 10^{-3} < d_{32} < 2.005 \times 10^{-3}$ m), and surface temperatures up to 400°C,

$$q''_{\text{trans}} = q''_{\text{CHF}} - \frac{q''_{\text{CHF}} - q''_{\text{min}}}{(\Delta T_{\text{CHF}} - \Delta T_{\text{min}})^3}[\Delta T^3_{\text{CHF}} - 3\Delta T^2_{\text{CHF}}\Delta T_{\text{min}} + 6\Delta T_{\text{CHF}}\Delta T_{\text{min}}\Delta T - 3(\Delta T_{\text{CHF}} + \Delta T_{\text{min}})\Delta T^2 + 2\Delta T^3] \tag{3}$$

where

$$q''_{\text{CHF}} = 122.4\rho_g h_{fg} Q''\left[1 + 0.0118\left(\frac{\rho_g}{\rho_f}\right)^{0.25}\left(\frac{\rho_f c_{pf}\Delta T_{\text{sub}}}{\rho_g h_{fg}}\right)\right] \times \left(\frac{\sigma}{\rho_f Q''^2 d_{32}}\right)^{0.198} \tag{4}$$

and

$$\Delta T_{\text{CHF}} = T_{\text{CHF}} - T_f = 18\left[(\rho_g h_{fg} Q'')\left(\frac{\sigma}{\rho_f Q''^2 d_{32}}\right)^{0.198}\right]^{0.180} \tag{5}$$

and q''_{min} and ΔT_{min} are given in Eqs. (6) and (7) for dilute sprays ($Q'' < 3.5 \times 10^{-3}$ m^3 s^{-1} m^{-2}),

$$q''_{\text{min}} = 33.244 \times 10^5 Q''^{0.544} u_m^{0.324} \tag{6}$$

$$\Delta T_{\text{min}} = 204.895 Q''^{0.066} u_m^{0.138} d_{32}^{-0.035} \tag{7}$$

Reviews of the literature have revealed that while there have been several qualitative and quantitative studies of the transition boiling characteristics of droplets and sprays, a comprehensive model that possesses the ability to accurately model and predict the transition boiling heat transfer rate of a complex spray is still unavailable. The object of the present study is to construct a spray transition boiling heat transfer correlation based on the heat transfer characteristics of a single droplet stream and the statistical droplet distributions of sprays. To achieve this goal, quantitative assessments are made regarding the significance of droplet diameter, droplet velocity, and surface temperature on the transition boiling heat transfer rate for a single stream of impinging droplets. The empirical correlations that capture these quantitative assessments are then combined with a basic analytical spray heat transfer model to arrive at a semiempirical model for the transition boiling heat flux of a spray. Finally, the spray heat transfer model is compared to empirical spray transition boiling heat transfer correlations to demonstrate its effectiveness and limitations.

Experimental Apparatus and Procedures

Figure 2 displays the experimental apparatus used to study the transition boiling heat transfer from a heated surface to a controlled single stream of water droplets. The apparatus is comprised of a water delivery system, a droplet generator and associated electronics, a heater module with instrumentation, and a data acquisition system. Complete details for all of the experimental equipment can be found in Refs. [16,21], and thus only a brief summary is given here.

The droplet generator [16–19], developed to produce monodispersed droplets, was equipped with one of four stainless steel orifice plates possessing orifice diameters of 0.130×10^{-3} m, 0.249×10^{-3} m, 0.343×10^{-3} m, and 0.533×10^{-3} m, to produce droplets with respective diameters of 0.244×10^{-3} m, 0.468×10^{-3} m, 0.645×10^{-3} m, and 1.002×10^{-3} m [21]. The droplet generation process is achieved by forcing liquid through a narrow orifice to develop a laminar jet, which is then mechanically vibrated over a narrow frequency range and forced to disintegrate into a periodic stream of uniformly sized droplets. Rayleigh [20] demonstrated that an axisymmetric disturbance, whose wavelength is greater than the circumference of the laminar jet, would overcome surface tension forces and cause the jet to break up into

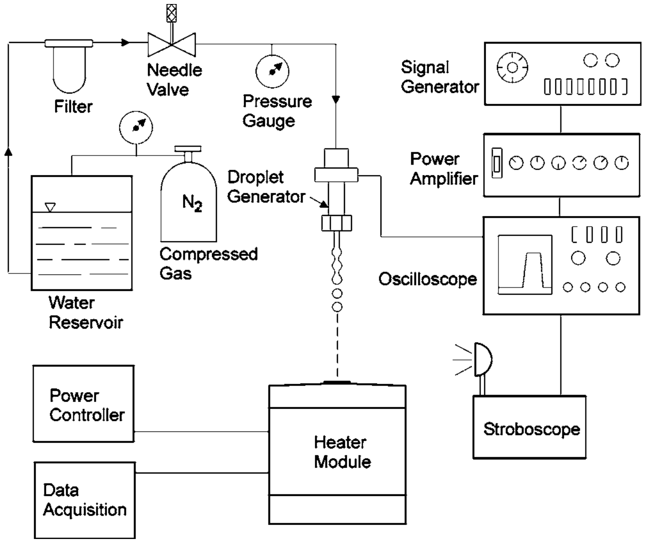

Fig. 2 Droplet heat transfer apparatus

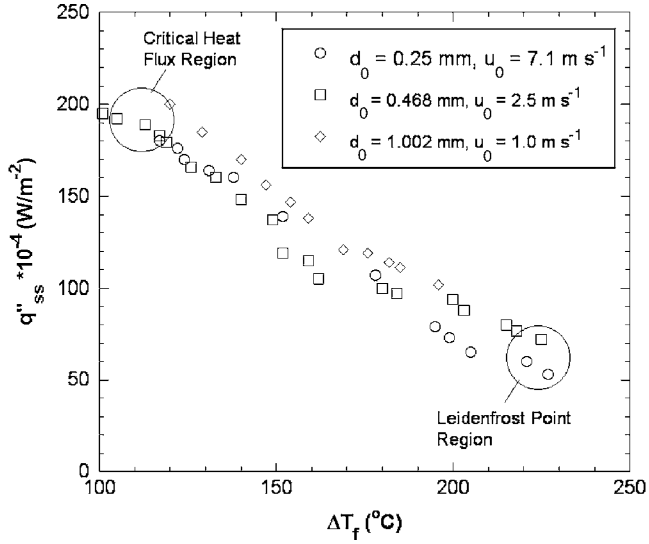

Fig. 3 Empirical data of heat flux from a heated surface to a single stream of droplets with a given diameter and velocity

a series of uniform droplets. Bernardin and Mudawar [16] showed that the optimum jet breakup frequency f_0 can be related to the droplet velocity u_0, droplet diameter d_0, most unstable wavelength λ_{opt}, or jet diameter D by

$$f_0 = \frac{u_0}{\lambda_{opt}} = \frac{u_0}{2.35 d_0} = \frac{u_0}{4.44 D} \tag{8}$$

A piezoceramic crystal, powered by a signal generator and power amplifier, was used to produce the mechanical vibrations for the droplet generator. As shown in Fig. 2, an oscilloscope was connected to the output of the power amplifier to precisely determine the electric field frequency. Furthermore, a strobe light, connected parallel to the output signal, was used to visually verify the successful breakup of the liquid jet into discrete droplets and to verify that the prescribed electrical disturbance frequency matched the droplet frequency. As discussed in Ref. [16], the droplet velocity was set by adjusting the flow rate to the generator for a given orifice diameter. This droplet generation technique created very stable and consistent droplet streams where no droplet-droplet interaction was witnessed prior to impact with the heated surface.

Table 1 summarizes the mean droplet diameters, velocities, and frequencies used in this study. Droplet diameters and velocities were measured with a Kodak Ektapro 1000 video motion analyzer in conjunction with a 200 mm zoom lens and a graduated ruler. Measured droplet diameters and velocities were within 10% and 5%, respectively, of the values listed in Table 1.

Table 1 Single droplet stream test parameters

Test number	$d_o \times 10^3$ (m)	$Q_{ss} \times 10^9$ ($m^3\,s^{-1}$)	u_o ($m\,s^{-1}$)	f (s^{-1})
1	0.250	40	3.0	5218
2	0.250	63	4.8	8311
3	0.250	78	5.8	10,162
4	0.250	94	7.1	12,327
5	0.468	74	1.5	1372
6	0.468	97	2.0	1817
7	0.468	120	2.5	2233
8	0.645	144	1.6	1032
9	0.645	177	1.9	1265
10	1.002	227	1.0	432
11	1.002	253	1.1	481

The heater module was designed to measure the heat transfer rate to a single stream of droplets impinging upon the polished nickel-plated surface. Wrapped around the circumference of the heater assembly was an electrical resistance heater (200 W at 120 V ac), which was powered by a variable ac voltage transformer. The heater assembly employed four calibrated type-K thermocouples (±0.2°C) to measure the heat conducted to the surface and dissipated by the droplet stream. The thermocouples, made from 0.076 mm (0.003 in.) diameter wires and inserted into 0.343 mm (0.135 in.) ceramic tubes, were placed at a depth of 3.99 mm (0.157 in.) and a spacing of 2.54 mm (0.10 in.). This heater configuration ensured a one-dimensional heat flow along the instrumented section [16,21]. A one-dimensional curve fit to the thermocouple readings allowed for an extrapolation of the surface temperature and heat flux. An error analysis based on uncertainties in geometry, thermocouple calibration values, copper thermal conductivity, and heat losses resulted in a maximum error of 7% in heat flux measurements [16,21].

Distilled water was used as the working fluid for all tests. To minimize the risk of contamination, the liquid was never recirculated in the flow apparatus. The clean fluid and intermittent repolishing of the test surface minimized the likelihood of changes in the heater surface conditions.

For a detailed description of the experimental test procedure, the reader is directed to Ref. [16].

Results

Experimental Measurements and Data Correlation. Figure 3 shows three data sets, typical of the experimental results obtained in this study. The plot displays the surface heat flux versus the temperature difference between the heater surface and the droplet for three different droplet stream conditions. These data sets encompass the transition boiling regime, from the CHF point to the Leidenfrost point. Additional data corresponding to the nucleate and film boiling regimes were obtained to identify the boundary points of the transition boiling regime but were omitted from Fig. 3 [16,21] for data correlation purposes.

Similar to the approach used in Ref. [16] for film boiling heat transfer, the transition boiling heat transfer rate for a single droplet stream was correlated in this study to the following form:

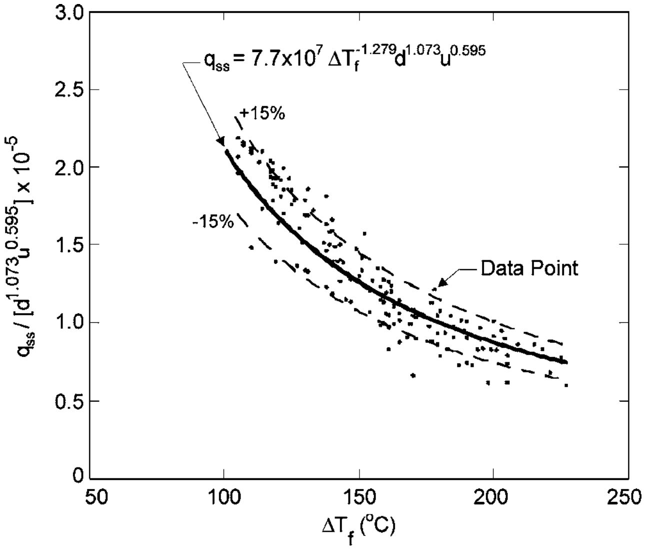

Fig. 4 Correlation of the single droplet stream transition boiling heat transfer rate data

$$q_{ss} = a_1 \Delta T_f^{a_2} d_0^{a_3} u_0^{a_4} \tag{9}$$

where a_1–a_4 are empirically determined coefficients. Using a linear least squares fitting technique, the following form of the correlation was obtained:

$$q_{ss} = 7.7 \times 10^7 \Delta T_f^{-1.279} d_0^{1.073} u_0^{0.595} \tag{10}$$

where q_{ss}, ΔT_f, d_0, and u_0 have the units of W, °C, m, and m s^{-1}, respectively. Figure 4 displays this correlation against the empirical data and indicates that the majority of the data lies within a +/−15% bracketed band about the correlation. Given this data scatter and the uncertainties in the droplet diameter, droplet velocity, and heat flux measurements, it is estimated that Eq. (10) has a mean uncertainty of 11%.

While Eq. (10) describes the transition boiling heat transfer rate to a droplet stream, it does not indicate the efficiency of the heat transfer process. Droplet heat transfer efficiency, as defined previously in Eq. (1), is the ratio of the actual to the maximum possible amount of heat transferred from a surface to a droplet. For a single droplet stream, this can be represented by

$$\varepsilon_{ss} = \frac{Q_{sd}}{Q_{max}} = \frac{q_{ss}}{f\rho_f \dfrac{\pi d_0^3}{6} h'_{fg}} \tag{11}$$

Substituting Eqs. (8) and (10) into Eq. (11) gives the transition boiling heat transfer efficiency of the single droplet streams investigated in this study,

$$\varepsilon_{ss} = \frac{3.46 \times 10^8}{\rho_f h'_{fg}} \Delta T_f^{-1.279} d_0^{-0.927} u_0^{-0.405} \tag{12}$$

Equation (12) corresponds to a closely packed or high frequency stream of droplets where a significant interference from successive drops occurs during the impact and heat transfer process on the heater surface. Consequently, the efficiency predicted by Eq. (12) will be lower than those obtained for single droplets or dilute sprays.

Equations (10) and (12) are valid for water droplet streams of uniform diameter, frequency, and velocity and for the following parametric ranges: $100 \leqslant \Delta T_f \leqslant 220°\mathrm{C}$, $0.250 \times 10^{-3} \leqslant d_0 \leqslant 1.002 \times 10^{-3}$ m, and $1.0 \leqslant u_0 \leqslant 7.1$ m s^{-1}

Dilute Spray Modeling and Assessment. In this section, the heat transfer correlation for a single droplet stream is incorporated into the development of a semiempirical model of the transition boiling heat flux for a dilute spray, q''_{sp}. A spray may be thought of, in a simplistic manner, as a series of droplet streams impinging upon a heated area. Furthermore, as pointed out in Ref. [16], it is reasonable to expect that the interaction between droplets in a spray will be different than in a droplet stream. Therefore, to model a spray as a series of droplet streams, a correction must be applied to account for differences in heat transfer efficiency of a spray and of a droplet stream. The entire mathematical development of this model and justification of the supporting arguments parallels that found in Ref. [16] for a similar model of spray film boiling, and thus the reader is directed to that reference for all of the supplementary information. Taking the approach outlined in Ref. [16], but employing the transition boiling expressions of Eqs. (10) and (12) of the present study, and replacing the single stream droplet diameters and velocities with, respectively, the spray Sauter mean diameter d_{32} and the spray mean droplet velocity u_m, the following transition boiling heat flux prediction for a dilute spray may be obtained:

$$q''_{sp,pred} = \rho_f h'_{fg} Q''_{sp} \varepsilon_{sd} \left(1 - \frac{Q''_{sp}}{Q''_{sp,dense}}\right) + 3.46 \times 10^8 \Delta T_f^{-1.279} d_{32}^{-0.927} u_m^{-0.405} \left(\frac{Q''^2_{sp}}{Q''_{sp,dense}}\right) \tag{13}$$

where the spray flux corresponding to a dense spray, $Q''_{sp,dense}$, was reported in Refs. [10,16] to be approximately 5×10^{-3} m^3 s^{-1} m^{-2}, as the lower limit for a fully dense spray.

The transition boiling heat transfer efficiency for a single impinging droplet, ε_{sd}, can be determined directly from Eq. (2). Another approach, which is more applicable to full cone water sprays, is to divide Eq. (3) by the maximum amount of heat transfer to a spray, $\rho f h'_{fg} Q''_{sp}$, and evaluate the result at a dilute volumetric spray flux of 0.175×10^{-3} m^3 s^{-1}m^{-2} [16]. This approach does not account for all aspects of droplet interference that could exist on a surface being exposed to a medium or dense spray. However, it is believed that these equations provide a reasonable characterization of a dilute spray.

Consequently, by knowing the single droplet heat transfer efficiency ε_{sd}, the spray parameters (d_{32}, u_m, Q''), and the excess surface temperature ΔT_f, Eq. (13) can be used to predict the local spray transition boiling heat flux. This model's predictive capability is best matched over the following parameteric ranges: $100 \leqslant \Delta T_f \leqslant 220°\mathrm{C}$, $0.250 \times 10^{-3} \leqslant d_{32} \leqslant 1.002 \times 10^{-3}$ m, and $1.0 \leqslant u_0 \leqslant 7.1$ m s^{-1}.

Figure 5 displays a comparison of the spray transition boiling heat flux model Eq. (13) versus two empirical spray transition boiling heat flux correlations [10,11] for a single set of spray parameters. Figure 5 allowed for the evaluation of two different methods that were used to calculate the single droplet heat transfer efficiency ε_{sd}, for Eq. (13). The first method included direct utilization of Eq. (2), which is the correlation by Deb and Yao [9]. The second method involved dividing Eq. (3) by the maximum amount of heat transfer to a spray, $\rho f h'_{fg} Q''_{sp}$, and evaluating the result at a dilute volumetric spray flux of 0.175×10^{-3} m^3 s^{-1} m^{-2}. As Fig. 5 indicates, the latter of these two methods yields a closer agreement between the spray heat flux model and the empirical correlations, and thus this approach was employed in all remaining model assessments. The disagreement between the heat flux model and the empirical correlation of Ref. [10] at low temperatures is explained in Fig. 6(*a*).

Figure 6 compares the spray transition boiling heat flux model Eq. (13) versus the empirical dilute spray heat flux correlation of Klinzing et al. [10] (Eq. (3)) for various spray fluxes, droplet diameters, and droplet velocities. Figure 6(*a*) shows an excellent agreement for the low volumetric spray flux (0.5×10^{-3} m^3 s^{-1} m^{-2}) and gradual departure in the agreement as the spray flux is increased. It appears that the model of Eq. (13) is applicable for very dilute sprays, but begins to lose its accuracy

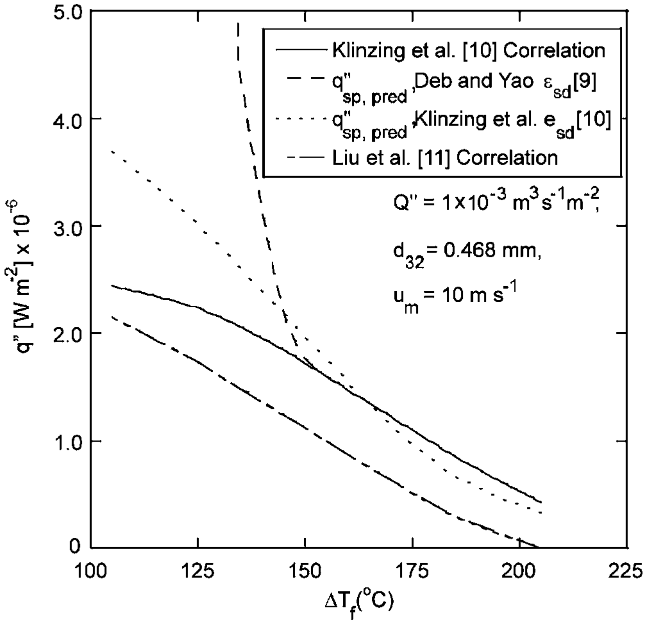

Fig. 5 Comparison of the spray transition boiling heat flux model to spray heat flux correlations

for spray fluxes greater than 1.0×10^{-3} m^3 s^{-1} m^{-2}. It is speculated that complex droplet interference and interaction effects, which occur in medium and dense sprays, can account for the limited capabilities of Eq. (13) [16]. Nevertheless, Fig. 6(*b*) and 6(*c*) indicate that the model's predictive capability is very good for droplet diameters and droplet velocities over the ranges of 0.250×10^{-3}–1.000×10^{-3} m and 5.0–15.0 m s^{-1}, respectively, for a volumetric spray flux of 0.5×10^{-3} m^3 s^{-1} m^{-2}.

Conclusions

This investigation focused on the transition boiling heat transfer rate and the heat transfer efficiency of a single stream of monodispersed water droplets. Furthermore, the study demonstrated how the complex behavior of spray transition boiling heat transfer can be modeled from fundamental observations of the controlled single droplet stream. From the experimental measurements and analytical modeling comparisons, the following key conclusions can be drawn.

1. Empirical correlations were developed for the transition boiling heat transfer rate and the heat transfer efficiency for a single stream of uniform droplets impinging upon a polished horizontal surface. The influential parameters for these correlations include droplet diameter, droplet velocity, and surface temperature.
2. By properly accounting for the hydrodynamic differences between a spray and a single droplet stream, the empirical single droplet stream heat transfer correlations were effectively extrapolated into a model for predicting the transition boiling heat flux of dilute sprays ($Q''\approx0.5\times10^{-3}$ m^3 s^{-1} m^{-2}).

Nomenclature

Symbol

c_p = specific heat (J kg^{-1} K^{-1})
D = laminar jet diameter (m)
d_o = droplet diameter (m)
d_{32} = droplet Sauter mean diameter (m)
f = frequency (s^{-1})
h_{fg} = latent heat of vaporization (J kg^{-1})

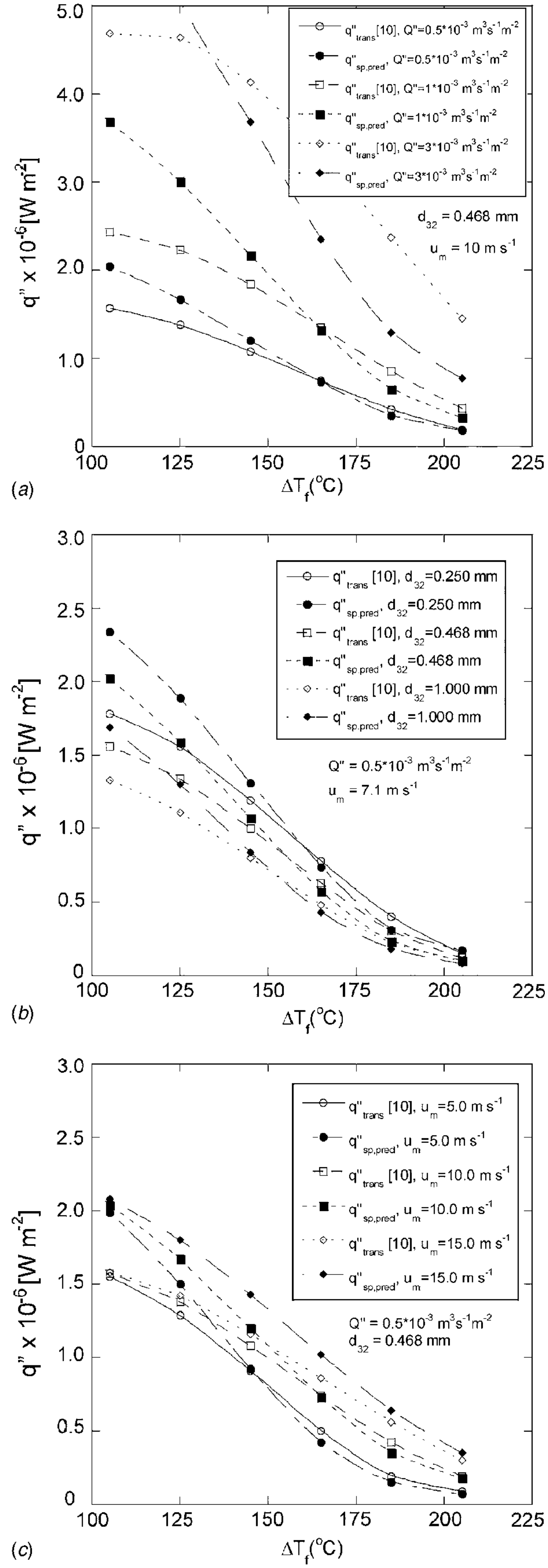

Fig. 6 Comparison of the spray transition boiling heat flux model, $q''_{\mathrm{sp,pred}}$, to the spray heat flux correlation of Klinzing et al. [10], q''_{trans}, for various (*a*) volumetric spray fluxes, (*b*) droplet diameters, and (*c*) droplet velocities

h'_{fg} = modified latent heat of vaporization $h_{fg}+c_{p,f}(T_{sat}-T_f)$ (J kg^{-1})
k = thermal conductivity (W m^{-1} K^{-1})
Q = total heat transfer (J), volume flow rate (m^3 s^{-1})
Q'' = volumetric spray flux (m^3 s^{-1} m^{-2})
q = heat transfer rate (W)
q'' = heat flux (W m^{-2})
T = temperature (°C)
T_{CHF} = temperature at CHF (°C)
T_{min} = temperature corresponding to minimum heat flux (°C)
u_o = droplet velocity (m s^{-1})
u_m = mean drop velocity in spray (m s^{-1})
We = Weber number, $(\rho u_o^2 d_o)/\sigma$

Greek Symbol

ΔT_{CHF} = $T_{CHF}-T_f$ (°C)
ΔT_f = T_s-T_f (°C)
ΔT_{min} = $T_{min}-T_f$ (°C)
ε = drop or spray heat transfer efficiency
λ = wavelength (m)
μ = dynamic viscosity (N s m^{-2})
ρ = density (kg m^{-3})
σ = surface tension (N m^{-1})

Subscript

CHF = critical heat flux condition
dense = dense spray condition
f = property of liquid
fg = difference between liquid and vapor
g = property of vapor
max = maximum
min = minimum heat flux or Leidenfrost point
pred = predicted
s = solid, surface
sat = saturation
sd = single droplet
sp = spray
ss = single droplet stream
trans = transition boiling

References

[1] Chandra, S., and Avedisian, C. T., 1991, "On the Collision of a Droplet With a Solid Surface," Proc. R. Soc. London, Ser. A, **432**, pp. 13–41.
[2] Inada, S., Miyasaka, Y., Nishida, K., and Chandratilleke, G. R., 1983, "Transient Temperature Variation of a Hot Wall Due to an Impinging Water Drop—Effect of Subcooling of the Water Drop," *Proceedings of the ASME-JSME Thermal Engineering Joint Conference*, Honolulu, HI, ASME, New York, Vol. 1, pp. 173–182.
[3] Takeuchi, K., Senda, J., and Yamada, K., 1983, "Heat Transfer Characteristics and the Breakup Behavior of Small Droplets Impinging Upon a Hot Surface," *Proceedings of the ASME-JSME Thermal Engineering Joint Conference*, Honolulu, HI, ASME, New York, Vol. 1, pp. 165–172.
[4] Makino, K., and Michiyoshi, I., 1984, "The Behavior of a Water Droplet on Heated Surfaces," Int. J. Heat Mass Transfer, **27**, pp. 781–791.
[5] Bernardin, J. D., Stebbins, C. J., and Mudawar, I., 1997, "Mapping of Impact and Heat Transfer Regimes of Water Drops Impinging on a Polished Surface," Int. J. Heat Mass Transfer, **40**, pp. 247–267.
[6] Bernardin, J. D., Stebbins, C. J., and Mudawar, I., 1997, "Effects of Surface Roughness on Water Droplet Impact History and Heat Transfer Regimes," Int. J. Heat Mass Transfer, **40**, pp. 73–88.
[7] Araki, K., Yoshinobu, S., Nakatani, Y., and Moriyama, A., 1982, "Stationary Measurement for Heat Transfer Coefficient in Droplet-Cooling of Hot Metal," Trans. Iron Steel Inst. Jpn., **22**, pp. 952–958.
[8] Senda, J., Yamada, K., Fujimoto, H., and Miki, H., 1988, "The Heat Transfer Characteristics of a Small Droplet Impinging Upon a Hot Surface," JSME Int. J., Ser. II, **31**, pp. 105–111.
[9] Deb, S., and Yao, S. C., 1987, "Heat Transfer Analysis of Impacting Dilute Spray on Surfaces Beyond the Leidenfrost Temperature," *Proceedings of the ASME National Heat Transfer Conference*, Pittsburgh, PA, ASME, New York, Vol. 1, pp. 1–8.
[10] Klinzing, W. P., Rozzi, J. C., and Mudawar, I., 1992, "Film and Transition Boiling Correlations for Quenching of Hot Surfaces With Water Sprays," J. Heat Treating, **9**, pp. 91–103.
[11] Liu, G. W., Morsi, Y. S., and Clayton, B. R., 2000, "Characterization of the Spray Cooling Heat Transfer Involved in a High Pressure Die Casting Process," Int. J. Therm. Sci., **39**, pp. 582–591.
[12] Choi, K. J., and Yao, S. C., 1987, "Mechanisms of Film Boiling Heat Transfer of Normally Impacting Spray," Int. J. Heat Mass Transfer, **30**, pp. 311–318.
[13] Yao, S. C., and Choi, K. J., 1987, "Heat Transfer Experiments of Mono-Dispersed Vertically Impacting Sprays," Int. J. Multiphase Flow, **13**, pp. 639–648.
[14] Mudawar, I., and Valentine, W. S., 1989, "Determination of the Local Quench Curve for Spray-Cooled Metallic Surfaces," J. Heat Treating, **7**, pp. 107–121.
[15] Delcorio, B., and Choi, K. J., 1991, "Analysis of Direct Liquid-Solid Contact Heat Transfer in Monodispersed Spray Cooling," J. Thermophys. Heat Transfer, **5**, pp. 613–620.
[16] Bernardin, J. D., and Mudawar, I., 1997, "Film Boiling Heat Transfer of Droplet Streams and Sprays," Int. J. Heat Mass Transfer, **40**, pp. 2579–2593.
[17] Brenn, G., and Frohn, A., 1993, "An Experimental Method for the Investigation of Droplet Oscillations in a Gaseous Medium," Exp. Fluids, **15**, pp. 85–90.
[18] Berglund, R. N., and Liu, B. Y., 1973, "Generation of Monodispersed Aerosol Standards," Environ. Sci. Technol., **7**, pp. 147–153.
[19] Anders, K., Roth, N., and Frohn, A., 1992, "Operation Characteristics of Vibrating-Orifice Generators: The Coherence Length," Part. Part. Syst. Charact., **9**, pp. 40–43.
[20] Rayleigh, L., 1878, "On the Instability of Jets," Proc. London Math. Soc., **10**, pp. 4–13.
[21] Bernardin, J. D., 1996, "Leidenfrost Point and Film Boiling Heat Transfer of Single Dropets and Sprays," Ph.D. thesis, Purdue University, West Lafayette, IN.